AIP | Applied Physics Letters

Optical performance of nanocrystalline transparent ceria films

P. Patsalas, S. Logothetidis, and C. Metaxa

Citation: Appl. Phys. Lett. **81**, 466 (2002); doi: 10.1063/1.1494458
View online: http://dx.doi.org/10.1063/1.1494458
View Table of Contents: http://apl.aip.org/resource/1/APPLAB/v81/i3
Published by the American Institute of Physics.

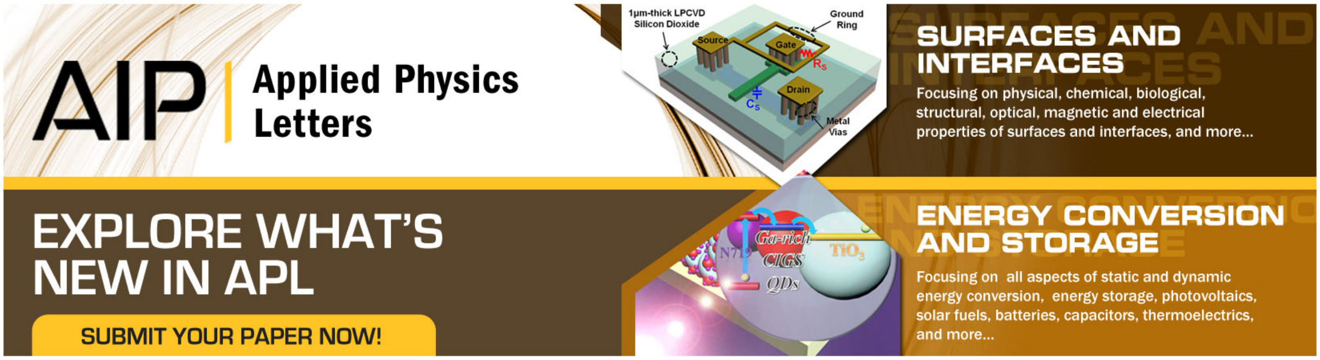

APPLIED PHYSICS LETTERS VOLUME 81, NUMBER 3 15 JULY 2002

Optical performance of nanocrystalline transparent ceria films

P. Patsalas,[a] S. Logothetidis, and C. Metaxa
Aristotle University of Thessaloniki, Department of Physics, GR-54006 Thessaloniki, Greece

(Received 30 November 2001; accepted for publication 21 May 2002)

Ceria is a transparent oxide suitable for various optical and optoelectronic devices. In this work, we tailor independently the refractive index n and fundamental gap E_g of nanocrystalline Ceria films by varying the substrate temperature or using Ar^+ ion beams during growth with electron beam evaporation. Spectroscopic ellipsometry and x-ray reflectivity are employed to study n and E_g and to identify the physical parameters that affect them. We correlate n (varies from 1.65 to 2.15 in the studied films) with the film density through a universal, square law. The film composition strongly affects E_g, which varies from 2.8 to ~2.0 eV. The optical absorption below 3 eV and the E_g shift are attributed to O-defect states and not to modifications in interband transitions. © *2002 American Institute of Physics.* [DOI: 10.1063/1.1494458]

Cerium dioxide ($\mathrm{CeO_2}$) or Ceria is a transparent oxide in the visible and near-IR spectral region. Thin films of Ceria exhibit physical properties such as fluorite structure with lattice constant ($a=0.541$ nm) similar to that of Si, high refractive index, and dc dielectric constant. Therefore, Ceria films are suitable for applications in optical,[1,2] electro-optical,[3,4] microelectronic,[5–8] and optoelectronic[9] devices.

Several deposition techniques have been used to grow Ceria films; among them is electron-beam evaporation (EBE).[1,5] Various reports have addressed the optical properties of Ceria films[1,4,7–10] providing different values for the refractive index n (from 1.6 to 2.5 at 633 nm), and the fundamental gap E_g. The reported results are qualitatively contradictory; e.g., the substrate temperature T_s has been reported either to decrease[1] or increase[4] n. Therefore, there is still a need for the accurate determination and the ability to tailor E_g and n of Ceria films, which are essential for their use in optical and optoelectronic devices.

In this work, the optical properties of nanocrystalline (grains of 8–40 nm) Ceria films are correlated with their microstructure. In addition, we show that their E_g and n can be tailored accordingly. The optical properties of Ceria/Si were studied by spectroscopic ellipsometry (SE) data analysis with the Tauc–Lorentz (TL) model.[11] The film microstructure was studied by x-ray photoelectron spectroscopy (XPS), x-ray diffraction (XRD) and reflectivity (XRR).[12] We found that the EBE deposition at room temperature (RT) results to films with $E_g=2.4$ eV and $n\sim1.65$, while Ceria films deposited with $T_s=950\,°\mathrm{C}$ exhibit $E_g=2.8$ eV and $n=2.15$. The refractive index has been explicitly correlated with the film density according to the classical dispersion theory,[13] revealing that density is the key factor to vary n. On the other hand, the film composition and microstructure affects E_g, as it has been shown by comparing films produced by EBE and ion beam assisted deposition (IBAD).

Ceria films, 110–170 nm thick, were deposited by EBE on c-Si(001) substrates in an ultrahigh vacuum chamber (base pressure $<1\times10^{-9}$ Torr) at various T_s (RT-950 °C) using a 40–50 mA/7 kV electron beam. Additional Ceria specimens were produced by IBAD (subsequent EBE deposition and bombardment with a 50 mA/0.75–1.25 keV Ar^+ ion beam using a Kauffman ion source). The optical properties of the deposited films were measured at RT by a phase modulated spectroscopic ellipsometer in the spectral range 1.5–5.5 eV with a step of 20 meV at 70° angle of incidence. XRR/XRD experiments were conducted in a Siemens D-5000 diffractometer, equipped with a Goebel mirror, in Bragg–Brentano geometry.[12] XRR scans with 0.1° detector offset were conducted to subtract the contribution of the scattered radiation from the specular scan.

Experimental XPS results (not presented) have shown that the average $x=[\mathrm{O}]/[\mathrm{Ce}]$ ratio is of the order of 1.9 for the studied films. XPS determined the O deficiency in the films from the fraction of trivalent Ce^{+3}, which corresponds to $\mathrm{Ce_2O_3}$. The amount of the $\mathrm{Ce_2O_3}$ varied from ~10% to ~5%, decreasing with T_s. XRD identified only the fluorite crystal structure of $\mathrm{CeO_2}$ (with the same cell size with bulk $\mathrm{CeO_2}$),[14] suggesting that the $\mathrm{Ce_2O_3}$ phase is amorphous. This phase is possibly located around the grain boundaries of the nanocrystalline Ceria, as its content decreases with increasing grain size.

SE measures the ellipsometric angles Ψ and Δ from which the complex dielectric function $\tilde{\varepsilon}\ (\omega)\ (=\varepsilon_1(\omega)+i\varepsilon_2(\omega))$ can be determined. In the case of transparent Ceria films, the measured quantity is the pseudodielectric function $\langle\tilde{\varepsilon}(\omega)\rangle$, which also takes into account the thickness of the film due to the multiple reflections from the film–substrate interface. In order to evaluate the dielectric function of each Ceria film itself, the $\langle\tilde{\varepsilon}(\omega)\rangle$ were fitted using a model of 2-TL oscillators (electronic transitions),[11] which determines E_g as well as the energy position E_o, broadening and strength of each oscillator, in combination with the three-phase model (air/film/Si) which takes into account the film thickness and the substrate contribution to the measured Ψ and Δ.[13]

Figure 1 shows the measured Ψ (circles) and Δ (triangles) spectra from a representative Ceria film, 160 ± 5 nm thick, deposited by EBE at RT on Si (100) and the corresponding results of the 2-TL fitting (solid line Ψ, and dash

---

[a] Electronic mail: ppats@skiathos.physics.auth.gr

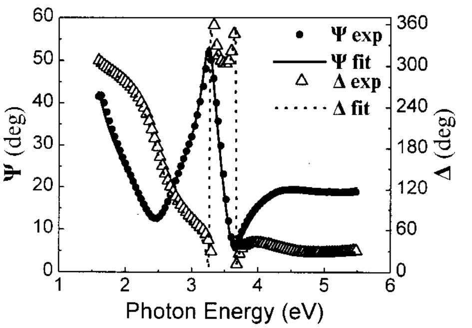

FIG. 1. The measured Ψ and Δ angles from a representative, EBE-produced Ceria film and the corresponding results of the fitting with the 2-TL model.

line Δ). The TL oscillators are located at $E_o \sim 4$ and ~ 8 eV and correspond to the $2p \rightarrow 4f$ and $2p \rightarrow 5d$ interband transitions,[15] respectively. The $n(\omega)$ and extinction coefficient $k(\omega)$ were calculated from $\tilde{\varepsilon}(\omega)[=(n+ik)^2]$, using the values of best-fit parameters, and they are shown in Fig. 2 for the two marginal cases of Ceria films deposited by EBE at RT and 950 °C. The n,k values for $E<1.5$ eV are the extrapolation of the TL-model results. The film deposited at 950 °C exhibits higher $n(\omega \sim 0)=2.15$ and $E_g \sim 2.8$ eV, than the film deposited at RT, which exhibits $n(\omega=0)=1.65$ and $E_g \sim 2.4$ eV. The difference in n is mainly attributed to the film density. It has been also found that the values of n for $E<E_g$ are not affected by the surface roughness (3–4 nm) of the films. The values of E_g have been determined by the TL model and they are smaller than those reported in literature.[10] This is a typical underestimation of E_g when the TL model is used, due to the Urbach tails in optical absorption, which are caused by defect states in the gap.[11] The real E_g values are estimated to be about 0.5 eV higher, as it was observed in thicker films, grown with similar conditions, using Tauc plots. We found that E_g decreases with increasing Ce^{+3} content in EBE films. This is in agreement with earlier works reporting that the O deficiency in bulk $\mathrm{CeO_2}$ induces optical absorption below 3 eV.[15] In addition, the IBAD-produced film, which is more O deficient than the film deposited by EBE at 950 °C and consists of smaller grains, exhibits smaller gap $E_g \sim 2.1$ eV, though it is dense and exhibits high $n=2.05$. This shows that we can tailor n and E_g independently and that there is no direct correlation between them.

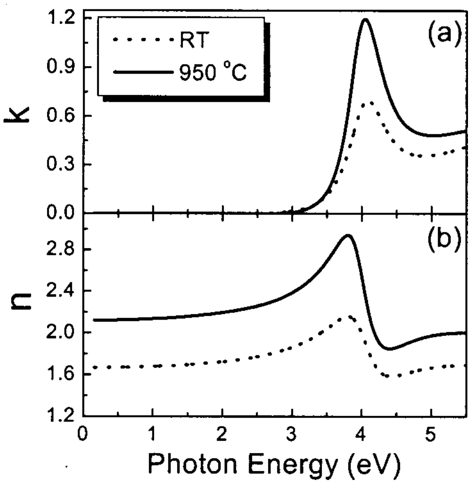

FIG. 2. The calculated $k(\omega)$, $n(\omega)$ for two Ceria films deposited at RT and 950 °C, based on the results of the 2-TL fitting.

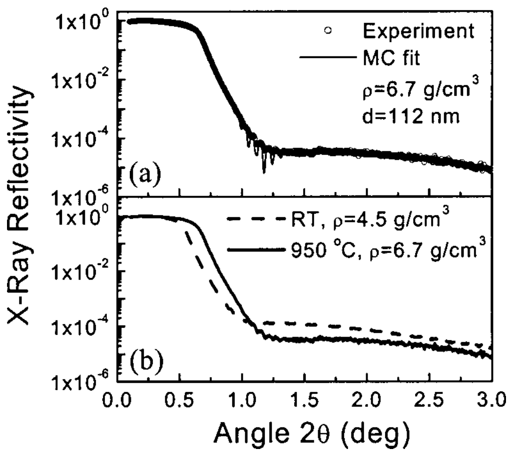

FIG. 3. (a) XRR data from a Ceria film deposited at 950 °C and the results of the MC fitting, and (b) comparison of XRR data of Ceria films deposited at RT and 950 °C.

The film density ρ was calculated by XRR from the critical angle for total reflection θ_c.[12] The XRR data were analyzed by the Siemens/RefSim Software and a Monte Carlo (MC) algorithm.[12] Figure 3(a) shows the XRR curve and the results of the MC fitting for a Ceria film, 112 nm thick, deposited at 950 °C. The calculated density (6.7 $\mathrm{g/cm^3}$) is smaller than the density of bulk Ceria (7.12 $\mathrm{g/cm^3}$)[14] and is even lower (4.5 $\mathrm{g/cm^3}$) for films deposited at RT as it is illustrated in Fig. 3(b). Figure 4 shows the variation of density (triangles) and n at $E=0.1\ \mathrm{eV} \ll E_g$ (squares), based on the extrapolation of the TL-model results, for Ceria films versus T_s.

The strong correlation of n with ρ (Fig. 4) is well explained by the classical theory of light dispersion.[13] The real part of the dielectric function of a material, which exhibits q electronic transitions, is given by

$$\varepsilon_1(\omega)=1+\frac{4\pi N_e e^2}{m}\sum_{k=1}^{q}\frac{f_k\cdot(\omega_k^2-\omega^2)}{(\omega_k^2-\omega^2)^2+\gamma_k^2\omega^2}, \tag{1}$$

where N_e is the total density of electrons and f_k, ω_k, and γ_k are the strength, frequency, and broadening of the kth transition, respectively. The f_k follows the sum rule: $\Sigma_{k=1}^{q} f_k = 1$. Then, n is associated with ε_1 through the relation $\varepsilon_1 = n^2 - k^2$ (for $\hbar\omega < E_g$, $k=0$, and $\varepsilon_1 = n^2$).[13] Finally, for ω

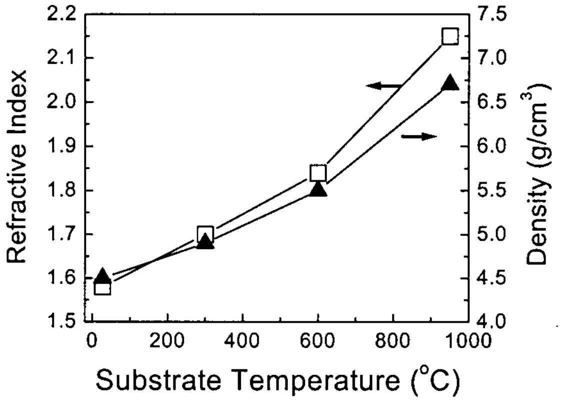

FIG. 4. The variation of the refractive index (open squares) and density (solid triangles) of EBE-produced films vs T_s.

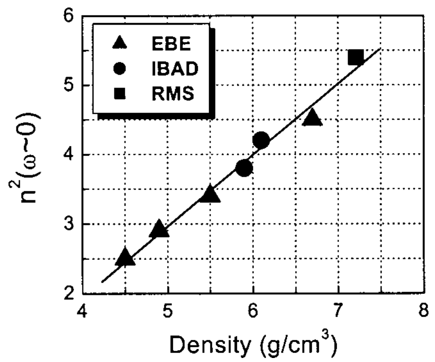

FIG. 5. The square of n vs ρ of Ceria films. The solid line is a fit with Eq. (2).

$\ll\omega_k$ and γ_k and taking into account that the electron density is associated with the mass density ρ through the relation $N_e = N_o(Z\rho/A)$ (N_o is Avogadro's number and A and Z the atomic mass and atomic number, respectively), we conclude that

$$n^2(\omega\approx 0) = 1 + \left(\frac{4\pi N_o Z e^2}{mA}\sum_{k=1}^{q}\frac{f_k}{\omega_k^2}\right)\cdot\rho. \tag{2}$$

$\Sigma_{k=1}^{q} f_k/\omega_k^2$ reflects the bandstructure of the material, through the strength and energy positions of the interband transitions.

The square of n follows a universal linear relation with ρ, as it is presented in Fig. 5, for films deposited by EBE, IBAD, and reactive magnetron sputtering (RMS)—the RMS point has been determined by applying the presented model to the optical data of crystalline Ceria reported by Guo *et al.*,[10] assuming that the density of the single crystal is equal to that of bulk Ceria (7.21 g/cm^3). We note here, however, that Eq. (2) and the SE results account only for the effect of the electronic transitions and do not include the contribution of bond vibrations, which are manifested in the IR region (275 cm^{-1}).[15] The linear relation between n^2 and ρ suggests, according to Eq. (2), that $\Sigma_{k=1}^{q} f_k/\omega_k^2$ remains almost the same for all Ceria films. Therefore, the O deficiency does not considerably affect the interband transitions of Ceria and the absorption tail below 3 eV is rather due to the defect absorption, which is induced by states within the gap.

In conclusion, we independently tailored the fundamental gap and the refractive index of nanocrystalline Ceria films by varying the substrate temperature or using Ar$^+$ ion beams during EBE growth. SE and XRR were employed to study the optical constants of Ceria films and to identify the factors that affect them. n varies from 1.65 to 2.15 in the studied films and follows a universal, explicit correlation between n and the film density, valid for both EBE and IBAD. The Ce_2O_3 variations strongly affect E_g, e.g., it is 2.4 and 2.8 eV for EBE films at RT and 950 °C, respectively. The optical absorption below 3 eV and the E_g shift are mainly attributed to the defect states and not to modifications of interband transitions.

[1] G. Atanassov, R. Thielsch, and D. Popov, Thin Solid Films **223**, 288 (1993).
[2] R. P. Netterfield, W. G. Sainty, P. J. Martin, and S. H. Sie, Appl. Opt. **24**, 2267 (1985).
[3] N. Ozer, Sol. Energy Mater. Sol. Cells **68**, 391 (2001).
[4] M. G. Krishna, A. Hartridge, and A. K. Bhattacharya, Mater. Sci. Eng., B **55**, 14 (1998).
[5] T. Inoue, M. Osonoe, H. Tohda, M. Hiramatsu, Y. Yamamoto, A. Yamanaka, and T. Nakayama, J. Appl. Phys. **69**, 8313 (1991).
[6] L. Tye, N. A. El-Masry, T. Chikyow, P. McLarty, and S. M. Bedair, Appl. Phys. Lett. **65**, 3081 (1994).
[7] D. P. Norton, J. D. Budai, and M. F. Chilsom, Appl. Phys. Lett. **76**, 1677 (2000).
[8] L. Mechin, A. Chabli, F. Bertin, M. Burdin, G. Rolland, C. Vanuffel, and J.-C. Villegier, J. Appl. Phys. **84**, 4935 (1998).
[9] A. H. Morshed, M. E. Moussa, M. Bedair, R. Leonard, S. X. Liu, and N. El-Masry, Appl. Phys. Lett. **70**, 1647 (1997).
[10] S. Guo, H. Arwin, S. N. Jacobson, K. Jarrendahl, and U. Helmersson, J. Appl. Phys. **77**, 5369 (1995).
[11] G. E. Jellison and F. A. Modine, Appl. Phys. Lett. **69**, 371 (1996).
[12] P. Patsalas and S. Logothetidis, J. Appl. Phys. **90**, 4725 (2001).
[13] F. Wooten, *Optical Properties of Solids* (Academic, New York, 1972).
[14] JCPDS Powder Diffraction File 43-1002.
[15] F. Marabelli and P. Wachter, Phys. Rev. B **36**, 1238 (1987).